Asian Biomedicine Vol. 5 No. 3 June 2011; 345-352 **DOI: 10.5372/1905-7415.0503.045**

Original article

Downregulation of p-ERK1/2 and p-AKT expression by curcumin and tetrahydrocurcumin in hepatocellular carcinoma-induced tumors in nude mice

Pornphrom Yoysungnoen Chintana[a], Ponthip Wirachwong[b], Apichart Suksamrarn[c], Suthiluk Patumraj[d]
[a]Division of Physiology, Faculty of Medicine, Thammasat University, Pathumthani 12120; [b]The Government Pharmaceutical Organization, Rama VI, Rajtevi, Bangkok 10330; [c]Department of Chemistry, Faculty of Science, Ramkhamhaeng University, Bangkok 10240; [d]Department of Physiology, Faculty of Medicine, Chulalongkorn University, Bangkok 10330, Thailand

Background: Curcumin (CUR) and tetrahydrocurcumin (THC) inhibits tumor angiogenesis. It is suggested that tumor progress may be related to the pathway of extracellular signal-regulated kinase 1/2 (ERK1/2) and serine/threonine kinase AKT, but the mechanism remains unclear.
Objective: Investigate the effects of CUR and THC on the expression of ERK1/2 and AKT in hepatocellular carcinoma (HepG2)-induced tumors in nude mice.
Methods: The curcuminoid mixture was obtained from the rhizomes of *Curcuma longa*, which was subjected to silica gel column chromatography to afford CUR as the major constituent. THC was prepared by hydrogenation of curcumin with palladium on charcoal as a catalyst. HepG2-implanted nude mice model was used to study of angiogenesis and tumor progression. Expressions of phospho-ERK1/2 (p-ERK1/2) and phopho-AKT (p-AKT) in HepG2-implated tissue were measured by immunohistochemistry. Tumor area, area of expression and expression ratio of pERK1/2 and p-AKT were determined.
Results: Increases in p-ERK1/2 and p-AKT expression in HepG2 group was related to changes in tumor growth in control, CUR, and THC groups. THC-treatment could attenuate the p-ERK1/2, p-AKT expression, tumor area, and ratio of expression in HepG2-implanted nude mice significantly, compared to CUR-treatment.
Conclusion: HepG2-induced tumor progression may be inhibited by THC in part through the inhibition of mitogen-activated protein kinase (MEK)/ERK and phosphoinositide 3-kinase (PI3K)/AKT.

Keywords: Curcumin, extracellular signal-regulated kinase 1/2, protein kinase B, tetrahydrocurcumin

Hepatocellular carcinoma (HCC) develops with neovascularization in tumors. Many molecular signaling molecules may be involved in the regulation of tumor development and angiogenesis. Recent studies have shown that tumor development and angiogenesis may be related with the pathway of extracellular signal-regulated kinase 1/2 (ERK1/2) and serine/threonine kinase AKT [1]. The ERK pathway is a cascade of mitogen-activated protein kinase, which is activated by vascular endothelial growth factor (VEGF) [2]. Activated-ERK1/2 mediates many cellular fates including growth, proliferation, and survival. The AKT pathway plays a vital role in cell proliferation, differentiation, and survival [3]. According to Schmitz et al. [4], increase in phospho-ERK1/2 (pERK1/2) and AKT expression in HCC indicates aggressive tumor behavior. Therefore, an appropriate target for cancer therapeutics is to explore drugs that inhibit or down-regulate the ERK and AKT pathways.

Hepatocellular carcinoma (HepG2)-implanted nude mice are an animal model for *in vivo* studies of tumor development and angiogenesis. In a previous

Correspondence to: Assist. Prof. Pornphrom Yoysungnoen Chintana, Division of Physiology, Faculty of Medicine, Thammasat University, Pathumthani 12120, Thailand. E-mail: pornprom_y@hotmail.com

study [5], we directly observed capillary network on the surface of tumors induced by HepG2 in a dorsal skin chamber of nude mice, using intravital fluorescence video-microscopy. The capillary density measured increased significantly during tumor development 7, 14, and 21 days after HepG2 implantation. In addition, the capillary density was reduced by supplementation of curcumin (CUR) or tetrahydrocurcumin (THC) [6]. This indicated that CUR and THC might be potent inhibitors of tumor angiogenesis because of their anti-oxidant activities.

It is reasonable to assume that the ERK and AKT pathways might play an essential role in dynamical process of tumor progress under supplementation of CUR and THC. However, no data are available for change in the expression of ERK1/2 and AKT during tumor development. In this study, we investigated effects of CUR and THC on ERK1/2 and AKT expression in HepG2-implanted nude mice. Based on image analysis of immunohistochemical stained tumor sections, we evaluated ERK1/2 and AKT expression 7, 14, and 21 days after HepG2 implantation.

Materials and methods

CUR and THC preparation

The curcuminoid mixture was obtained from the rhizomes of *Curcuma longa*, which was subjected to silica gel column chromatography, using hexane-dichloromethane, dichloromethane, and dichloromethane-methanol as eluents to afford CUR as the major constituent. THC was synthesized from CUR by catalytic hydrogenation reaction, with palladium on charcoal as a catalyst. The product was purified by silica gel column chromatography followed by recrystallization with dichloromethane-hexane to give 75% yield of THC [7].

HepG2-implanted nude mice

Forty BALB/c-nude mice (male, 20-25 g) from National Laboratory Animal Center of Salaya Campus, Mahidol University, Thailand were used for this study. The nude mice were bred and maintained in a specific pathogen germ-free environment. The animal experiment was conducted according to the guideline of experimental animals by the National Research Council of Thailand.

The nude mice were divided into four groups:
1) Controls supplemented with dimethyl sulfoxide (DMSO (Con; n=10),
2) HepG2-implanted mice supplemented with DMSO (HepG2+DMSO; n=10),
3) HepG2-implanted mice supplemented with CUR (HepG2+CUR, n=10),
4) HepG2-implanted mice supplemented with THC (HepG2+THC, n=10).

According to the procedure reported previously [5], we prepared 30 HepG2-implanted nude mice. Briefly, after anesthesia with sodium pentobarbital (50 mg/100 g body weight, *i.p.*), we implanted a dorsal skin-fold chamber (7 mm in diameter) into the upper layer of skin in a mouse. We inoculated 30 mL HepG2 cells (American Type Culture Collection, 2 10^6 cells, viability 95-97%) into the middle area of the chamber. Then, the mice were housed at one animal per cage, where sterile water and standard laboratory chow were freely accessed.

For the HepG2+CUR or HepG2+THC groups, the mice were daily supplemented with CUR or THC (2 mL of 3,000 mg/kg body weight) dissolved in 0.1% DMSO. The supplement was started 24 hours after inoculation of HeG2 cells.

Tissue sections for histolopgical examination

Parts of tissue within a dorsal skin chamber were isolated from mice 7, 14, and 21 days after HepG2 implantation. The isolated tissue was fixed in 10% buffered neutral formalin solution, and embedded in paraffin wax. The solid sections were cut at 5 μm, deparaffinized in xylene, and hydrated using graded series of alcohol.

For each section with 5 μm thickness, endogenous peroxidase activity was blocked with 3% hydrogen peroxide for 15 minutes at room temperature. After washing in water, non-specific binding sites were blocked with 1% bovine serum in phosphate buffer solution (PBS) for 30 minutes at room temperature. Then, the section was incubated overnight at 4^{O}C with specific primary antibody for phospho-AKT (p-AKT) (1:100 dilution), or phospho-ERK1/2 (p-ERK1/2) (1:200 dilution) (Cell Signaling Tech, Beverly, USA).

The section was washed with PBS for five minutes, and incubated with diluted biotinylated secondary antibodies (1:200, Vector Laboratories, Burlingame, USA) for 30 minutes at room temperature. The specificity of the p-AKT or p-ERK1/2 antibodies was confirmed in incubation without the p-AKT or p-ERK1/2 antibody, respectively.

The stained sections were developed with 0.03% diaminiobenzidine (DAB) as substrate, in a dark room

for 10 minutes, counter-stained with hematoxylin followed by dehydration, mounted under coverslips with permount, and dried adequately.

Image analysis

The stained sections were used for image analysis under a light microscope at magnification 10x. Using ImageJ 1.38 software (National Institutes of Health, USA), we calculated areas of tumors, activated p-ERK1/2 and p-AKT expression according to the procedure shown in **Figure 1**. These are 1) Convert color image (**A**) of sample to grayscale 8-bit images (**B**), 2) Set measurement scale by draw a line over a 100 μm section of the ruler, then *Analyze* → *Set Scale*, 3) threshold of grayscale image was adjusted by manual settings by Menu *Image* → *Adjust* → *Threshold* and outing of analyzed area will be draw (**C**), 4) Calculate the analyzed area by Menu *Analyze* → *Analyze particles*, then outline of entire area is automatically draw (**D**) and give a total area of each image (**E**).

One section with 5 μm thickness included several masses of tumors (see **Figure 1(A)**. The total areas of tumors, p-ERK1/2 expression, and p-AKT expression on one section were calculated, and the mean area of tumor (S, mm^2), p-ERK1/2 expression (S_{ERK}, mm^2), and p-AKT expression (S_{AKT}, mm^2) averaged over 20-sections of tissues were determined as follows:

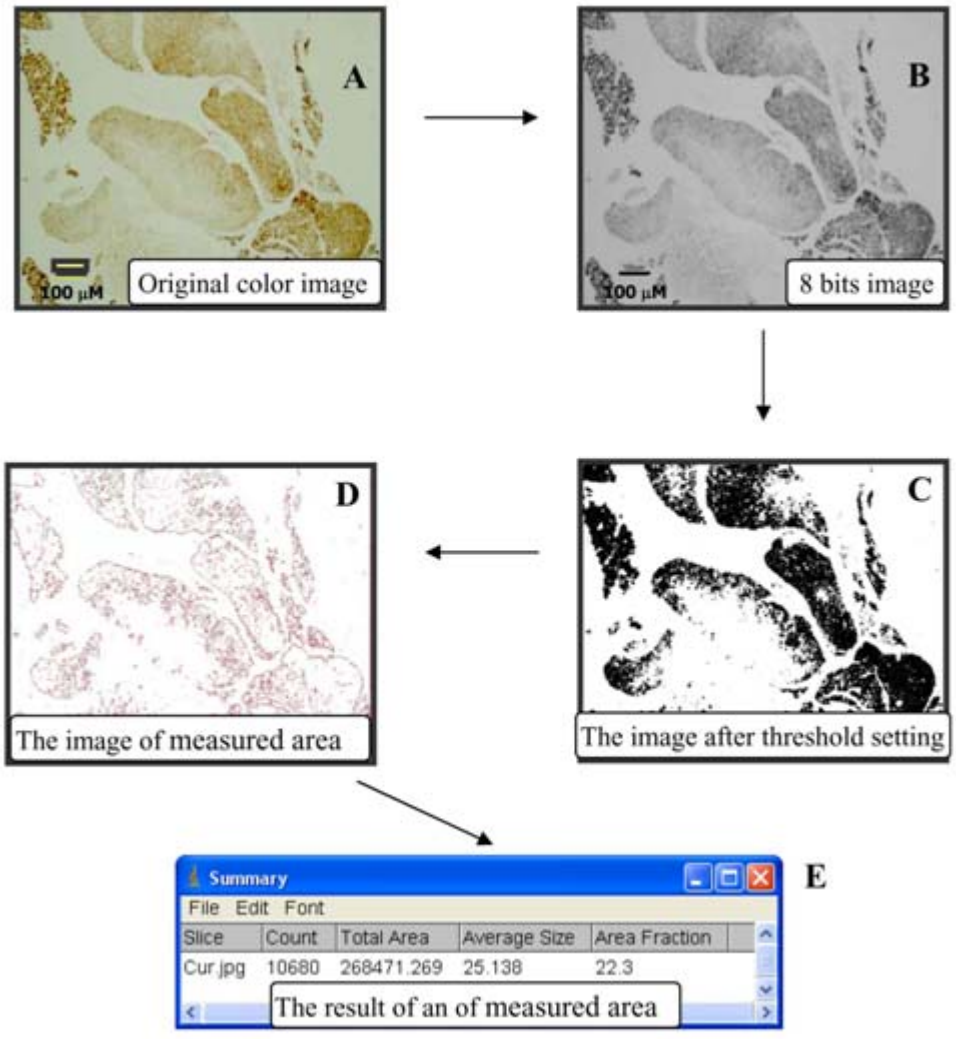

Figure 1. Schematic representation of the image analysis used to characterize the activated ERK1/2 and p-AKT expression area. (10x, Bar=100 μm.).

$$S = (1/N) \sum_{i=1}^{N}{}_{i} (\text{total area of tumor in each section}), \quad (1)$$

$$S_{ERK} = (1/N) \sum_{i=1}^{N}{}_{i} (\text{total area of tumor in each section}), \quad (2)$$

$$S_{AKT} = (1/N) \sum_{i=1}^{N}{}_{i} (\text{total area of ERK1/2 expression in each section}), \quad (3)$$

where N is number of slides used for image analysis. In the present analysis, 20 slide samples (N=20) were randomly selected in each mouse.

Percent area of S_{ERK} and S_{AKT} were determined using Eq (1) and (2), and Eq (1) and (3), respectively, as follows:

$$\% S_{ERK} = S_{ERK}/S \ (x100\%), \quad (4)$$
$$\% S_{ERK} = S_{ERK}/S \ (x100\%). \quad (5)$$

Statistical analysis

All data are presented as means ± standard error of mean (SEM). The data were analyzed by pair t-test and one-way ANOVA followed by the LSD test for comparisons of all pairs of groups. A p-value less than 0.05 was considered significant. All analyses were performed using SPSS version 13.0 (SPSS Inc, Chicago, USA).

Results

Figure 2 shows microscopic images of immunohistochemical stained sections for four groups (one control, three HepG2). HepG2 tumor sections exhibited p-ERK1/2 and p-AKT expression, while normal tissue exhibited no staining. The p-ERK1/2 and p-AKT expression revealed a specific positive nuclei immunostaining. Note that p-ERK1/2 and p-AKT expression were most marked in HepG2+DMSO group. CUR or THC supplementation reduced the over-expression of p-ERK1/2 and p-AKT.

Tumor area

Figure 3 shows the tumor area calculated by Eq. (1) for three HepG2 groups 7, 14, and 21 days after HepG2 implantation. We note that the tumor area increased with days after HepG2 implantation, and CUR or THC supplementation reduced the growth of tumor area.

Figure 4 shows the mean areas of ERK1/2 and AKT expression (S_{ERK} and S_{AKT}, mean±SEM) of each group calculated by Eq (2) and (3) on days 7, 14, and 21 after supplementation of DMSO, CUR or THC in HepG2 groups. The S_{ERK} and S_{AKT} have gradually increased from 7 to 21 day.

Figure 5 shows percent expression ratios of ERK1/2 and AKT ($\%S_{ERK}$ and $\%S_{AKT}$, mean±SEM) of each group calculated by Eq (4) and (5) on days 7, 14, and 21 after supplementation of DMSO, CUR, or THC in HepG2 groups. The $\%S_{ERK}$ and $\%S_{AKT}$ significantly increased in HepG2 group, but they were attenuated by both high dose treatments with CUR and THC. Interestingly, THC treatment shows a significant attenuate area of p-ERK1/2 and p-AKT expression than CUR, suggesting that THC has more potential than CUR on suppression of activated ERK1/2 and AKT.

Discussion

In this study, we investigated the expression of p-ERK1/2 and p-AKT to assess the effectiveness of CUR and THC in HepG-induced tumors in nude mice. We assumed that p-ERK1/2 and p-AKT were expressed in tumor cell nuclei on immunohistochemical stained sections. By counting number of positively stained pixels, we measured the areas of tumors, p-ERK1/2 expression, and p-AKT expression over 20 images per each mouse and 200 images per each group.

In the present experiment, increases in p-ERK1/2 and p-AKT expression might be closely related with and changes in tumor growth in control, CUR, and THC groups, as shown in **Figures 3** and **5**. This result agrees with previous reports [4, 8-9] showing that increased pERK1/2 and AKT expression was associated with aggressive tumor behaviors in hepatocellular carcinoma. According to recent studies by Jiang et al. [3, 10], PI3K, and AKT play a key role in regulating tumor growth and angiogenesis through

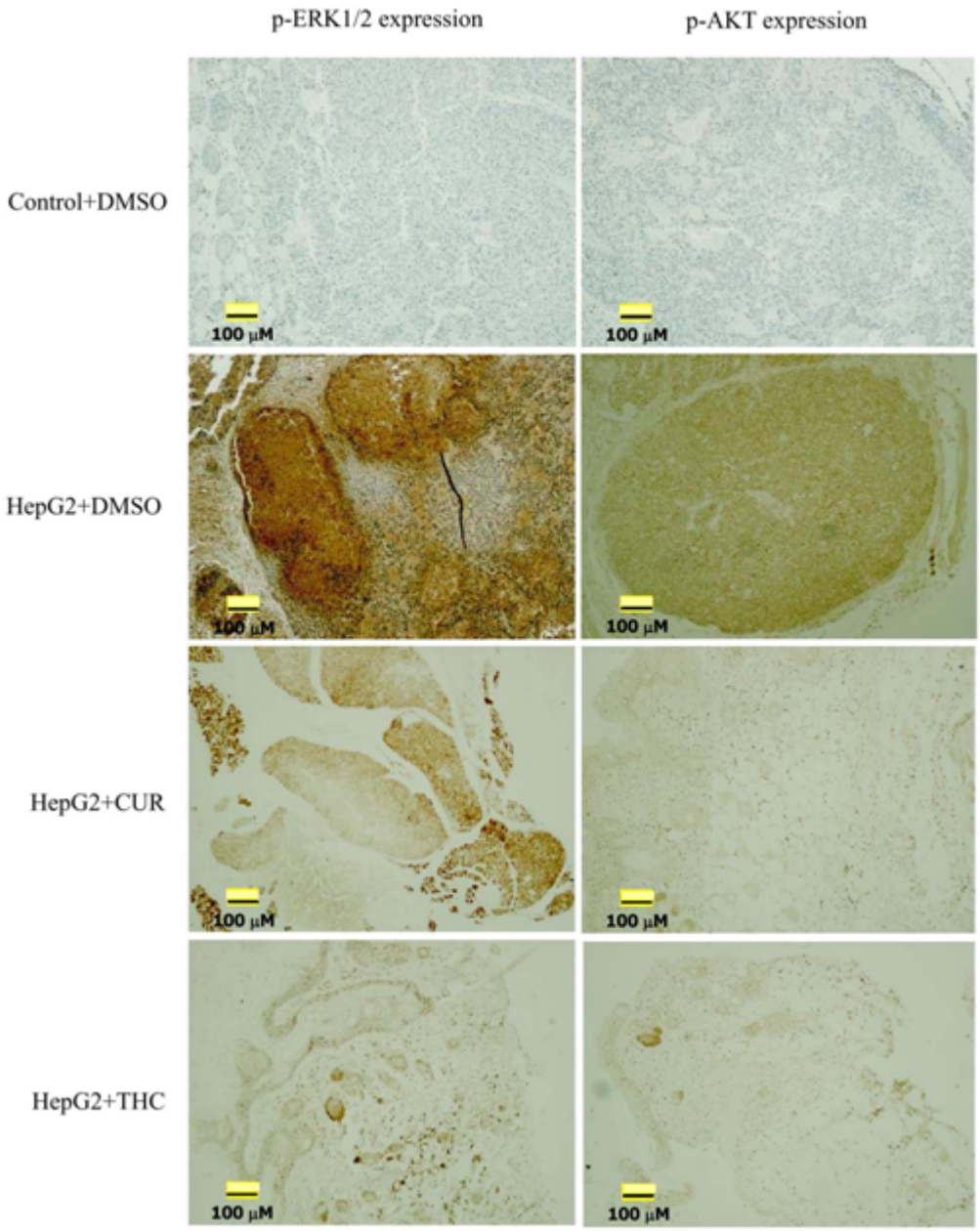

Figure 2. Immunohistochemical-stained images showing p-ERK1/2and p-AKT expressions in control group, HepG2+DMSO, HepG2+CUR and HepG2+THC group on day 21. (10x, Bar=100 μm.).

VEGF and HIF-1 expression, while the MEK/ERK signaling pathway induces NF- κB activation to regulate angiogenesis. Therefore, our task is to develop drugs that inhibit or down-regulate the ERK and AKT pathway for cancer therapy.

The present results demonstrated that THC could inhibit p-ERK1/2 and p-AKT expression, and expression ratio (**Figures 4** and **5**), which may be associated with the tumor area (**Figure 3**). In previous study [11], we showed that CUR could inhibit several angiogenic biomarkers such as VEGF and cyclooxygenase-2 (COX-2) expression. Recently, Roskoski et al. [2] and Namkoong et al. [12] showed that VEGF stimulating pathway is dependent upon activating the MAP kinase/ERK and PI3K/AKT pathway. Since MAP kinase/ERK and PI-3/AKT pathways influence COX-2 stimulating pathway [13], they should be involved in the mechanism for CUR to inhibit tumor angiogenesis and tumor progression. Although CUR is an important anti-cancer and anti-

angiogenic agent, the molecular mechanism of CUR activities remains unclear. Sharma et al. [14] made clinical studies of oral CUR (phase I) and revealed that low systemic bioavailability followed oral dosing. This reason might be that the ultimate metabolites of CUR were not used. In fact, substantial beneficial effects could be achieved with lower levels of these active metabolites compared to the parent compounds.

THC is a reduced analog of CUR with phenolic and β-diketo moieties as well as CUR. THC is valued as the ultimate metabolites of CUR *in vivo*. According to Sugiyama et al. [15], the β-diketone moiety may play an important role in the elucidation of anti-mutagenesis or anti-carcinogenesis. In addition, β-diketone type antioxidants such as n-tritriacontan-16,18-dione (TTAD) have been reported to inhibit tumor promotion and carcinogenesis [16]. THC may be more effective than CUR *in vivo* because THC is more easily absorbed and resistant to hydrolysis than CUR from gastrointestinal tract [17].

In conclusion, THC markedly decreased the MEK/ERK and PI3K/AKT expression associated with its inhibition of HepG2-induced tumor in nude mice model. Our data provide a potential role for THC in the pathogenesis of tumor progression.

Acknowledgements

This study was supported by the Thailand Research Fund (No. MRG5180092). The authors have no conflict of interest to declare.

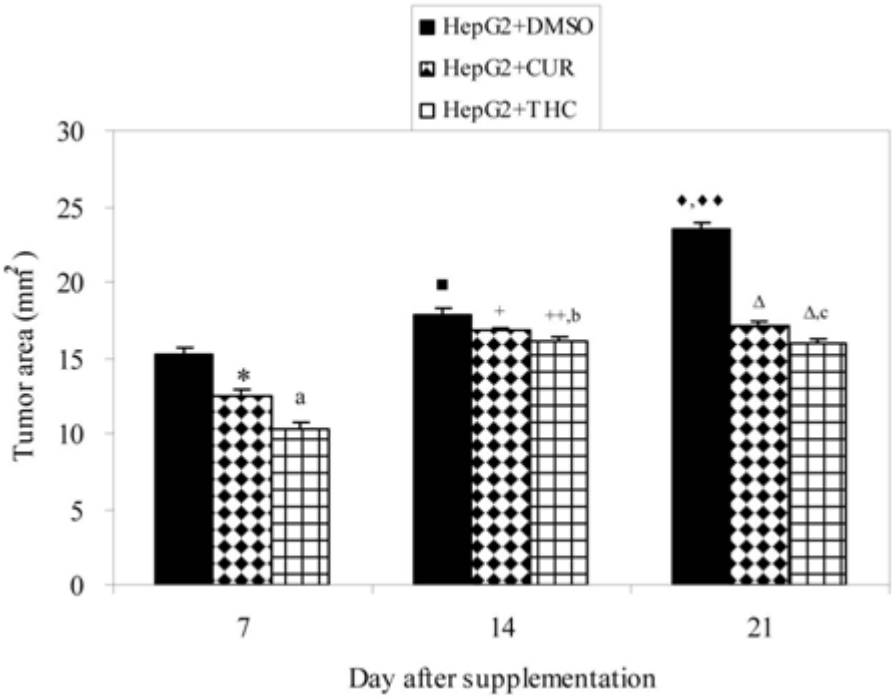

Figure 3. Tumor area (mean±SEM) of HepG2, HepG2+CUR, HepG2+THC groups on days 14 and 21 after supplementation of DMSO, CUR or THC. *p <0.001 *vs*. HepG2 with vehicle on day 7, [a]p <0.001 *vs*. HepG2+CUR on day 7, [%]P <0.05 *vs*. HepG2 with vehicle on day 7,[♦]p <0.001 *vs*. HepG2 with vehicle on day 7, [♦♦]p <0.001 *vs*. HepG2 with vehicle on day 14, [+]p <0.01 *vs*. HepG2 with vehicle on day 14, [++]p <0.001 *vs*. HepG2 with vehicle on day 14, [b]p <0.05 *vs*. HepG2+CUR on day 14, [Δ]p <0.001 *vs*. HepG2+DMSO on day 21, [c]p <0.01 *vs*. HepG2+CUR on day 21.

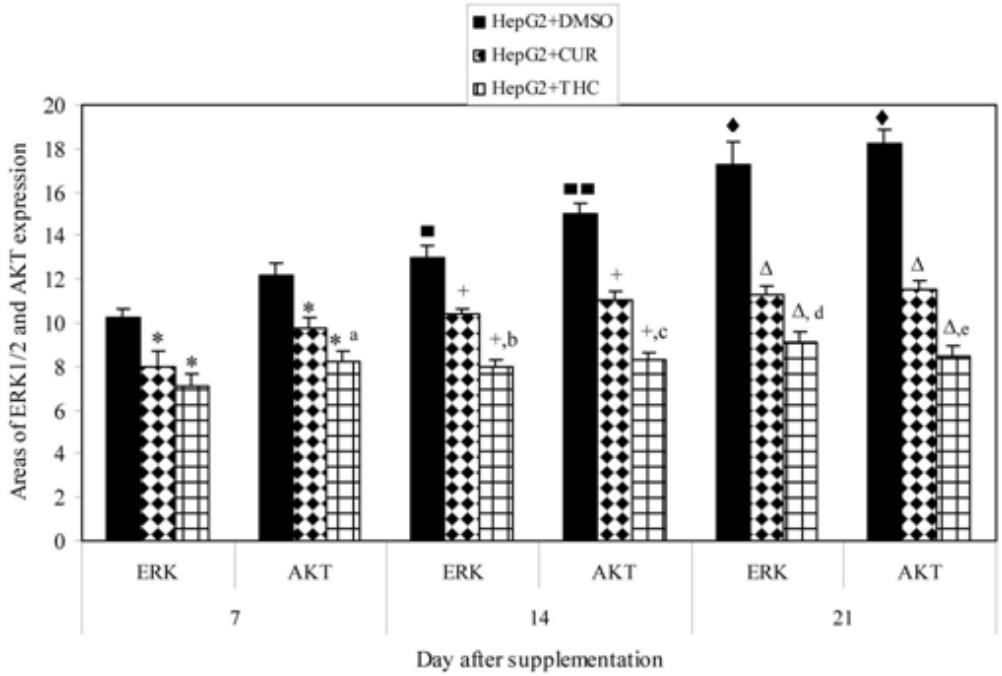

Figure 4. Area of ERK1/2 and AKT expression (mean±SEM) of HepG2, HepG2+CUR, HepG2+THC groups on days 7, 14, and 21 after supplementation of DMSO, CUR, or THC. *p <0.001 *vs*. HepG2 with vehicle on day 7, [a]P <0.05 *vs*. HepG2+CUR on day 7, [%]P <0.005 *vs*. HepG2 with vehicle on day 7, [%%]p <0.001 *vs*. HepG2 with vehicle on day 7, [f&]p <0.005 *vs*. HepG2 with vehicle on day 14, [+]P <0.001 *vs*. HepG2 with vehicle on day 14, [b]p <0.05 *vs*. HepG2+CUR on day 14, [c]p <0.005 *vs*. HepG2+CUR on day 14, [Δ] p <0.001 *vs*. HepG2 with vehicle on day 21, [d]p <0.05 *vs*. HepG2+CUR on day 21, [e]p <0.005 *vs*. HepG2+CUR on day 21.

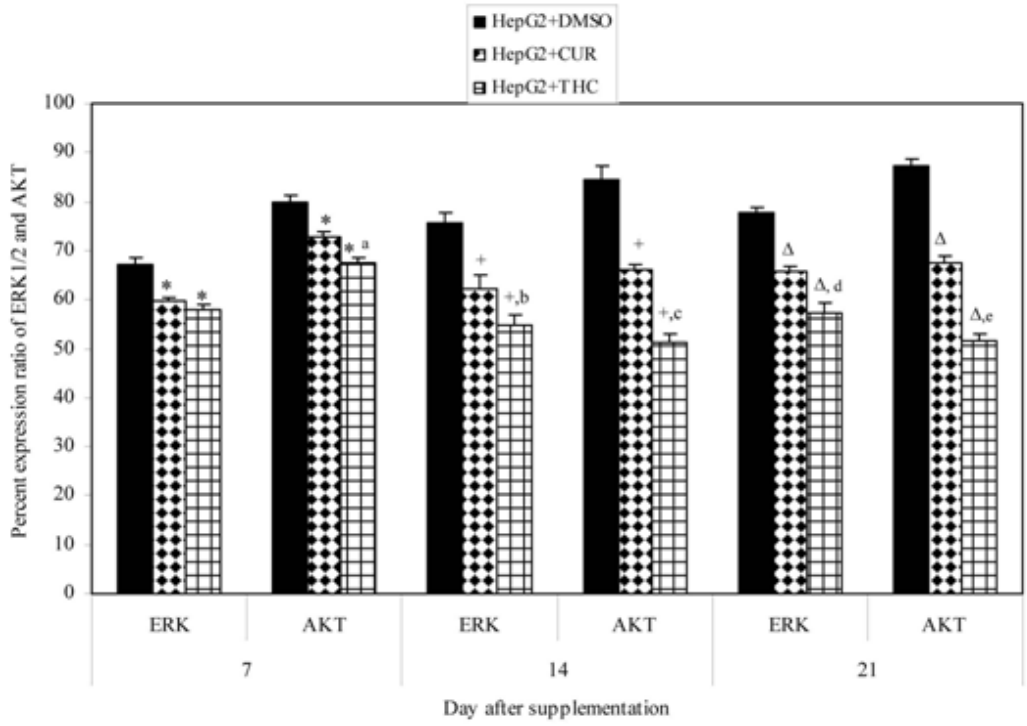

Figure 5. Expression ratio (mean±SEM) of ERK1/2 and AKT in HepG2, HepG2+CUR, HepG2+THC groups on days 7, 14, and 21 after supplementation of DMSO, CUR or THC. *P <0.001 *vs.* HepG2 with vehicle on day 7, [a]p <0.05 *vs.* HepG2+CUR on day 7, [+]p <0.001 *vs*. HepG2 with vehicle on day 14, [b]p <0.005 *vs.* HepG2+CUR on day 14, [c]p <0.001 *vs*. HepG2+CUR on day 14, [Δ]p <0.001 *vs*. HepG2 with vehicle on day 21, [d]p <0.005 *vs*. HepG2+CUR on day 21, [e]p <0.001 *vs*. HepG2+CUR on day 21.

References

1. Sebolt-Leopold JS, Herrera R, Ohren JF. The mitogen-activated protein kinase pathway for molecular-targeted cancer treatment. Recent Results Cancer Res. 2007; 172:155-67.
2. Roskoski JR. Vascular endothelial growth factor (VEGF) signaling in tumor progression. Critical Reviews in Oncology/Hematology. 2007; 62:179-213.
3. Jiang BH, Liu LZ. PI3K/PTEN signaling in angiogenesis and tumorigenesis. Adv Cancer Res. 2009; 102:19-65.
4. Schmitz KJ, Wohlschlaeger J, Lang H, Sotiropoulos GC, Malago M, Steveling K, Reis H, Cicinnati VR, Schmid KW, Baba HA. Activation of the ERK and AKT signalling pathway predicts poor prognosis in hepatocellular carcinoma and ERK activation in cancer tissue is associated with hepatitis C virus infection. J Hepatol. 2008; 48:83-90.
5. Yoysungnoen P, Wirachwong P, Changtam C, Suksamrarn A, Patumraj S. Suppression of tumor neocapillarization induced by HepG2 cells in nude mice supplemented with curcumin or tetrahydrocurcumin: An in vivo comparative study. Asian Biomed. 2008; 2:77-82.
6. Yoysungnoen P, Wirachwong P, Changtam C, Suksamrarn A, Patumraj S. Anti-cancer and anti-angiogenic effects of curcumin and tetrahydrocurcumin on implanted hepatocellular carcinoma in nude mice. World J Gastroenterol. 2008; 14:2003-9.
7. Lee SL, Huang WJ, Lin WW, Lee SS, Chen CH. Preparation and anti-inflammatory activities of diarylheptanoid and diarylheptylamine analogs. Bioorg Med Chem. 2005; 13:6175-81.
8. Tsuboi Y, Ichida T, Sugitani S, Genda T, Inayoshi J, Takamura M, Matsuda Y, Nomoto MAoyagi Y. Overexpression of extracellular signal-regulated protein kinase and its correlation with proliferation in human hepatocellular carcinoma. Liver Int. 2004; 24:432-6.
9. Wiesenauer CA, Yip-Schneider MT, Wang Y, Schmidt CM. Multiple anticancer effects of blocking MEK-ERK signaling in hepatocellular carcinoma. J Am Coll Surg. 2004; 198:410-21.
10. Jiang BH, Liu L-Z. PI3K/PTEN signaling in tumorigenesis and angiogenesis. Biochimica et al. Biophysica Acta (BBA) - Proteins & Proteomics. 2008; 1784:150-8.
11. Yoysungnoen P, Wirachwong P, Bhattarakosol P, Niimi H, Patumraj S. Effects of curcumin on tumor angiogenesis and biomarkers, COX-2 and VEGF, in hepatocellular carcinoma cell-implanted nude mice. Clin Hemorheol Microcirc. 2006; 34:109-15.
12. Namkoong S, Kim C-K, Cho Y-L, Kim J-H, Lee H, Ha K-S, Choe J, Kim P-H, Won M-H, Kwon Y-G, Shim EB, Kim Y-M. Forskolin increases angiogenesis through the coordinated cross-talk of PKA-dependent VEGF expression and Epac-mediated PI3K/Akt/eNOS signaling. Cellular Signalling. 2009; 21:906-15.
13. Agarwal S, Achari C, Praveen D, Roy KR, Reddy GV, Reddanna P. Inhibition of 12-LOX and COX-2 reduces the proliferation of human epidermoid carcinoma cells (A431) by modulating the ERK and PI3K-Akt signalling pathways. Exp Dermatol. 2009; 18:939-46.
14. Sharma RA, Euden SA, Platton SL, Cooke DN, Shafayat A, Hewitt HR, Marczylo TH, Morgan B, Hemingway D, Plummer SM, Pirmohamed M, Gescher AJ, Steward WP. Phase I clinical trial of oral curcumin: biomarkers of systemic activity and compliance. Clin Cancer Res. 2004; 10:6847-54.
15. Sugiyama Y, Kawakishi S, Osawa T. Involvement of the beta-diketone moiety in the antioxidative mechanism of tetrahydrocurcumin. Biochem Pharmacol. 1996; 52:519-25.
16. Takaba K, Hirose M, Yoshida Y, Kimura J, Ito N, Shirai T. Effects of n-tritriacontane-16, 18-dione, curcumin, chlorophyllin, dihydroguaiaretic acid, tannic acid and phytic acid on the initiation stage in a rat multi-organ carcinogenesis model. Cancer Letters. 1997; 113:39-46.
17. Okada K, Wangpoengtrakul C, Tanaka T, Toyokuni S, Uchida K, Osawa T. Curcumin and especially tetrahydrocurcumin ameliorate oxidative stress-induced renal injury in mice. J Nutr. 2001; 131:2090-5.